

Genetic isolation of stem cell-derived pacemaker-nodal cardiac myocytes

Sherin I. Hashem · William C. Claycomb

Received: 13 May 2013 / Accepted: 10 July 2013
© Springer Science+Business Media New York 2013

Abstract Dysfunction of the cardiac pacemaker tissues due to genetic defects, acquired diseases, or aging results in arrhythmias. When arrhythmias occur, artificial pacemaker implants are used for treatment. However, the numerous limitations of electronic implants have prompted studies of biological pacemakers that can integrate into the myocardium providing a permanent cure. Embryonic stem (ES) cells cultured as three-dimensional (3D) spheroid aggregates termed embryoid bodies possess the ability to generate all cardiac myocyte subtypes. Here, we report the use of a *SHOX2* promoter and a *Cx30.2* enhancer to genetically identify and isolate ES cell-derived sinoatrial node (SAN) and atrioventricular node (AVN) cells, respectively. The ES cell-derived *Shox2* and *Cx30.2* cardiac myocytes exhibit a spider cell morphology and high intracellular calcium loading characteristic of pacemaker-nodal myocytes. These cells express abundant levels of pacemaker genes such as endogenous *HCN4*, *Cx45*, *Cx30.2*, *Tbx2*, and *Tbx3*. These cells were passaged, frozen, and thawed multiple times while maintaining their pacemaker-nodal phenotype. When cultured as 3D aggregates in an attempt to create a critical mass that simulates in vivo architecture, these cell lines exhibited an increase in the expression level of key regulators of cardiovascular development, such as *GATA4* and *GATA6* transcription factors. In addition, the aggregate culture system resulted in an increase in the

expression level of several ion channels that play a major role in the spontaneous diastolic depolarization characteristic of pacemaker cells. We have isolated pure populations of SAN and AVN cells that will be useful tools for generating biological pacemakers.

Keywords Atrioventricular · Embryoid body · Embryonic stem cell · Sinoatrial · Pacemaker

Introduction

Cardiac arrhythmias and conduction abnormalities represent a major cause of world-wide morbidity and mortality [1]. Electronic pacemaker implants are effective in controlling arrhythmia, however they have numerous limitations. These limitations range from failing to pace, or irregular pacing to severe complications that can lead to patient mortality [2, 3]. This has prompted researchers to design biological pacemakers that could provide an alternative or adjunct to electronic pacemakers providing a potential permanent cure for the millions of patients suffering from arrhythmias [4].

Using the embryoid body (EB) differentiation system, all subtypes of cardiac myocytes develop and could be distinguished based on their morphological, molecular, and functional properties [5]. These embryonic stem (ES) cell-derived cardiac myocytes have been transplanted in vivo and have demonstrated the ability to functionally couple and pace host myocytes in animal models [6, 7]. However, no pure population of cardiac pacemaking myocytes has been cultured or propagated so far. The generation of pure pacemaker cell lines is critical for creating a cell-based therapy and for developing biological pacemakers.

Electronic supplementary material The online version of this article (doi:10.1007/s11010-013-1764-x) contains supplementary material, which is available to authorized users.

S. I. Hashem · W. C. Claycomb (✉)
Department of Biochemistry and Molecular Biology, Louisiana State University Health Sciences Center, 1901 Perdido Street, New Orleans, LA 70112, USA
e-mail: wclayc@lsuhsc.edu

Based on the fact that cardiac myocytes developing within EBs comprise all specialized cardiac cell subtypes such as atrial, ventricular, pacemaker-nodal, and Purkinje-fiber cells [5], we used ES cells to isolate pure populations of cardiac pacemaker-nodal cells. The sinoatrial node (SAN) is the primary pacemaker of the heart, and is responsible for generating the electric impulse [8, 9]. *Shox2*, a member of the short stature paired-homeodomain family of transcription factors, is a major genetic determinant of the SAN genetic pathway and is restrictedly expressed in the region of the SAN in vivo [10, 11]. We used a *SHOX2* promoter to isolate a population of SA pacemaker-nodal cells from differentiating EBs. The atrioventricular node (AVN) is the secondary pacemaker of the heart in cases of SAN failure or block [12, 13]. A minimal *Cx30.2* enhancer that delineates the AVN in vivo [14] was used to isolate AV pacemaker-nodal cells from differentiating EBs. Using a modified version of the genetic technique, first described by Klug et al. [15], we isolated *Shox2* (SAN) and *Cx30.2* (AVN) cells from EBs.

Materials and methods

Culture of ES cells

The mouse ES cell lines CJ-7 and *Shox2^{lacZ/+}* were cultured as previously described [16]. The cells were cultured in growth medium [DMEM supplemented with 15 % fetal bovine serum (FBS) (Sigma), 0.1 mM nonessential amino acids solution (NEAA), 100 U/ml penicillin, 100 µg/ml streptomycin, 2 mM L-glutamine, and 50 µM β-Mercaptoethanol (BME), containing 10³ U/ml leukemia inhibitory factor LIF (Millipore)]. The ES cells were passaged every 48 h. All cultures were grown in an atmosphere of 95 % air 5 % CO₂ at 37 °C.

Generation of EBs

A hanging drop technique was used to generate EBs as previously described [5]. Briefly, 20 µl drops of differentiation medium (DMEM supplemented with 10 % FBS, 0.1 mM NEAA, 100 U/ml penicillin, 100 µg/ml streptomycin, 2 mM L-glutamine, and 50 µM BME) each containing 500 ES cells were transferred onto non-treated Petri dishes. On day 5 of differentiation, EBs were plated onto culture dishes and were allowed to adhere and continue their differentiation until the day of the experiments.

Generation of *Cx30.2* enhancer-RFP construct

A 1.2 kb mouse *Cx30.2* enhancer specific to the AVN [14] was inserted into the *KpnI/BamHI* site in the multiple

cloning region of a promoter-less red fluorescent protein (RFP) vector (Evrogen). The *Cx30.2* enhancer-RFP segment was then excised and inserted into the *KpnI/EcoRV* site of the pcDNA3.1 (+) Hygro vector (Invitrogen). CJ-7 ES cells were transfected with the linearized *Cx30.2* enhancer-RFP construct using Lipofectamine LF2000 (Invitrogen) following the manufacturer's protocol. The cells were selected using hygromycin (Sigma) at a concentration of 300 µg/ml for 8 days.

Fluorescent live imaging

EBs were incubated in medium containing 20 µM fluorescein digalactoside (FDG-C12) (Molecular Probes) for 20 min at 37 °C. EBs were then washed with phosphate buffered saline (PBS) and incubated for 1 h in differentiation medium. For visualization, a Nikon (eclipse TE300) microscope was used. LacZ reporter expression was imaged using a FITC filter, and RFP reporter expression using a Rhodamine filter. Images were captured using a digital camera (Roper Scientific), and were analyzed using MetaMorph software (version 5.0 v6, Molecular Devices, Sunnyvale, CA).

Construction of selection vectors

A pcDNA3.1 (+) neo vector (Invitrogen) was previously modified by digestion with *BclI* and re-ligation. This resulted in the re-positioning of the neomycin resistance gene (*neo*) immediately downstream of the multiple cloning site [17]. To construct a *SHOX2-neo* vector, a 3.8 kb fragment of the *SHOX2* promoter [18] was inserted between the *NotI* and *HindIII* sites of the modified pcDNA3.1 (+) neo vector. To construct a *Cx30.2-neo* vector, a 1.2 kb fragment of a *Cx30.2* enhancer [14] was inserted between the *KpnI* and *AflIII* sites of the modified pcDNA3.1 (+) neo vector using a linker.

Isolation of *Shox2* cells and *Cx30.2* cells

CJ-7 ES cells were transfected with the linearized *SHOX2-neo* vector or linearized *Cx30.2-neo* vector. In order to enrich the population of cells containing the vectors, the ES cells were co-transfected with linear pcDNA3.1 (+) hygromycin using LF2000 following the manufacturer's protocol. Transfected ES cells were cultured for 7 days in growth medium containing hygromycin at a concentration of 300 µg/ml. These genetically modified ES cells were differentiated using a suspension protocol as previously described [15]. On day 8 of differentiation, EBs were dissociated using trypsin-EDTA for 5 min and the cell suspensions were transferred onto 0.1 % gelatin-coated

culture dishes. On the following day, neomycin “G418” (Invitrogen) at a concentration of 200 µg/ml was added to the two-dimensional (2D) cultures. Every other day, the cells were washed with PBS and fresh medium containing G418 at a concentration of 200 µg/ml was added for 7 days. The few remaining cells that survived selection were allowed to grow and expand for 10 days in the absence of G418. The cells were subjected to a second round of selection in medium containing G418 at a concentration of 200 µg/ml for another 7 days. The cells were then cultured in medium containing no G418 and were passaged every 4 days.

Generation of three-dimensional (3D) aggregates and co-culture

Shox2 cells or Cx30.2 cells were cultivated as hanging drops to generate 3D aggregates. Each drop contained 400 cells in 30 µl differentiation medium. The Petri dishes were inverted and incubated at 37 °C for 4 days. The aggregates were plated onto 0.1 % gelatin-coated culture plates until the day of the experiments. For co-culture experiments, the 3D aggregates were added to 2D HL-1 cell monolayer cultures at 50–70 % confluence. The co-cultures were left to grow for an additional 1–3 days. HL-1 cells were cultured as previously described [19].

Calcium imaging

For calcium imaging, cells were incubated in PBS containing 10 µM of Calcium Green (Invitrogen) for 20 min at 37 °C. The cells were then washed with PBS, and incubated for 1 h in differentiation medium. Visualization and image acquisition were performed using a Nikon Eclipse TE300 microscope and a digital camera. Analysis of images was performed using MetaMorph software.

Western blot analysis

Whole cell lysates were extracted from HL-1 cells, Shox2 cells, and Cx30.2 cells. Cell lysates were resolved by SDS-PAGE, transferred to PVDF, and immunoblotted with primary antibodies: Cx45 (1:1,000, Millipore), Cx30.2 (1:2,000, Invitrogen), HCN4 (1:500, Santa Cruz), α -sarcomeric actinin (1:1,000, Sigma), titin (1:1,000, Santa Cruz), MF20 (1:500, Santa Cruz), and anti- β -actin antibody (1:2,000, Abcam). Detection of signals was visualized using Super Signal West Pico Chemiluminescent Substrate (Pierce, Rockford, IL). ImageQuant LAS 4000 (GE Healthcare Life Sciences) was used for capturing the images.

Quantitative reverse transcriptase polymerase chain reaction (qRT-PCR)

Total RNA isolation, reverse-transcription, and qRT-PCR were performed as previously described [20]. The primers used are listed in Supplemental Table 1. Cycle thresholds (CT) were recorded and the $2^{-\Delta\Delta CT}$ algorithm was used to analyze the relative changes in gene expression as previously described [21]. GAPDH was used as an internal control.

Statistical analysis

Student’s *t* test and GraphPad Prism version 6 were used for statistical analysis. Data are expressed as mean \pm standard error of mean. *P* values smaller than 0.05 are considered significant.

Results and discussion

Identification of differentiating SAN and AVN cells in EBs

ES cells cultured as 3D EBs possess the ability to differentiate into every cardiac cell subtype [5]. To delineate the cells of the developing SAN in EBs, we used a live β -galactosidase assay and fluorescent imaging to visualize the reporter-positive cells in spontaneously contracting *Shox2*^{lacZ/+} EBs. We demonstrate that the reporter-positive cells form an organized cluster that is reproducibly located directly adjacent to the beating area in all contracting EBs examined ($n > 100$) (Fig. 1a; Supplemental online video 1). Using fluorescent imaging to visualize Cx30.2-RFP reporter expression in EBs, we demonstrate that reporter-positive cells organized in clusters that were always located within the beating area in all contracting EBs examined ($n > 20$) (Fig. 1b; Supplemental online video 2). Although, there is some heterogeneity with regard to the size of these reporter-positive cell clusters, the organization with respect to the contracting regions is consistent. Altogether, this data reveals that the *Shox2* gene and a *Cx30.2* enhancer identify discrete subpopulations of cells within contracting EBs. These reporter-positive cells are always associated with the spontaneously contracting region in EBs.

Isolation of Shox2 cells and Cx30.2 cells

To isolate a pure population of SA nodal cells from differentiating EBs, we generated ES cells stably transfected with a vector in which the neomycin resistance gene is under the control of a 3.8 kb region of the *SHOX2* promoter (Fig. 2a). This *SHOX2* promoter region contains

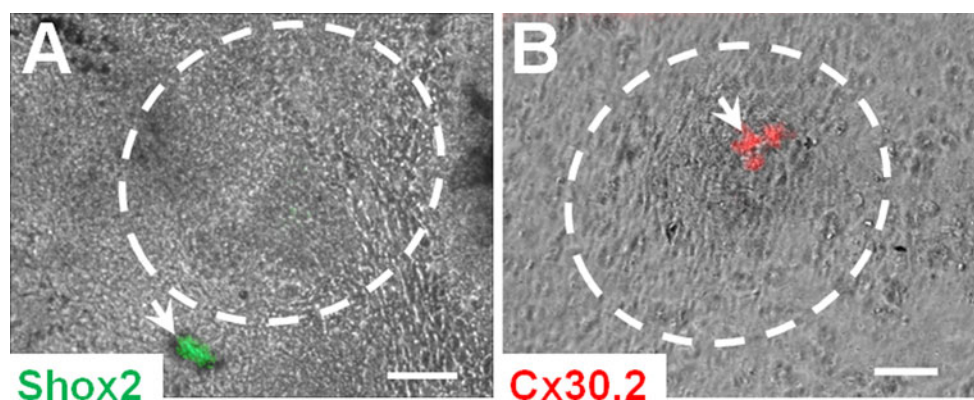


Fig. 1 A *Shox2* gene and a *Cx30.2*-enhancer identify discrete clusters of nodal cells in contracting EBs. **a** A representative live image of a *Shox2*^{lacZ/+} EB acquired using a fluorescence microscope following live fluorescein digalactoside staining. The EB is at day 11 of differentiation and shows visible contractions. The *Shox2* cell cluster (green) is located adjacent to the contracting region of the EB (area

surrounded by dashed circle) (Supplemental online video 1). **b** A representative live image of a *Cx30.2*-RFP EB acquired using a fluorescence microscope. The EB is at day 14 of differentiation and shows visible contractions. The *Cx30.2* cell cluster (red) is within the contracting region of the EB (area surrounded by dashed circle) (Supplemental online video 2) Bar 100 μ m. (Color figure online)

three putative *Tbx5* as well as three putative *Nkx2.5* binding sites [18]. To isolate a pure population of AV nodal cells from differentiating EBs, we generated ES cells stably transfected with a vector in which the neomycin resistance gene is under the control of a 1.2 kb region of a *Cx30.2* enhancer (Fig. 2b). This minimal *Cx30.2* enhancer contains putative *Tbx5* and *GATA4* binding sites [14]. EBs were generated using these genetically modified ES cells, and on day 8 of differentiation these EBs were dissociated into single cells and were subjected a day later to selection using G418 for 7 days (Fig. 2c). The dissociation of EBs prior to antibiotic selection insured adequate delivery of the selection drug to all of the cells. In addition, due to the fact that the population of cells we were selecting is very small, the dissociation of the EBs prior to treatment helped prevent excessive sloughing of layers of cells which can sometimes be associated with loss of healthy cells. The surviving G418-resistant *Shox2* and *Cx30.2* cells were propagated and expanded. These *Shox2* cells and *Cx30.2* cells grew in clusters (Fig. 2d, f) and exhibited spider cell morphologies (Fig. 2e, g). Cells isolated from the rabbit SAN have been shown to exhibit a similar spider cell morphology. These rabbit spider cells have a branched cytoplasm, and are weak in contractile proteins [22–24].

Isolated *Shox2* cells and *Cx30.2* cells exhibit high basal Ca^{2+} levels

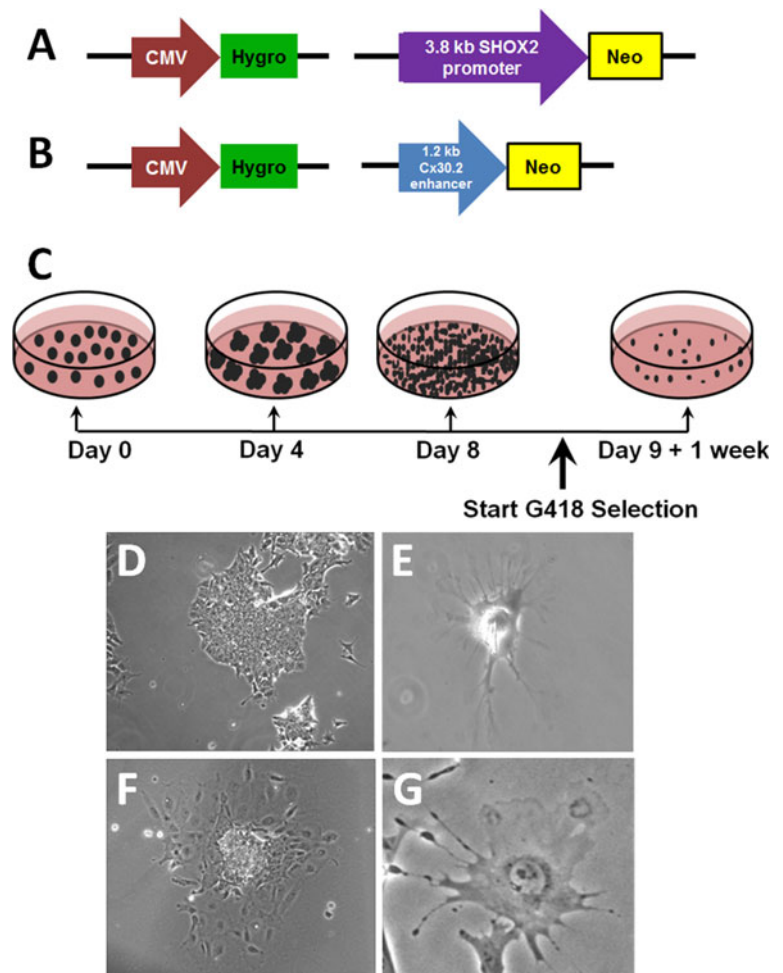
Ca^{2+} -dependent depolarizations play a major role in the generation of the cardiac pacemaker activity [25–28]. In recent years, studies have shown that the pacemaker rhythm is initiated, sustained, and regulated by oscillations in the release of intracellular Ca^{2+} from the sarcoplasmic reticulum (Ca^{2+} clock) [29, 30]. The sarcoplasmic

reticulum is the major Ca^{2+} store in cardiac pacemaker cells. The intracellular Ca^{2+} release regulates the normal automaticity of cardiac pacemaker cells and ignites excitation from within these cells [31, 32]. We used a fluorescent Ca^{2+} sensitive dye to assess spontaneous calcium transients in *Shox2* cells and *Cx30.2* cells. Live fluorescent imaging of the *Shox2* cells and the *Cx30.2* cells demonstrated the presence of a high basal level of Ca^{2+} ions characteristic of pacemaker cells (Fig. 3). *Shox2* and *Cx30.2* cells showed higher Ca^{2+} loading compared to control ES cells (Fig. 3a–f) and to HL-1 cells that were co-cultured with these cell lines (Fig. 3g, h). Taken together, this data indicate that *Shox2* and *Cx30.2* cells demonstrate the ability to concentrate Ca^{2+} which is characteristic of pacemaker cells [30, 31, 33, 34].

Characterization of gene expression profiles in *Shox2* cells

Using qRT-PCR, we examined the expression of 33 genes to characterize the molecular phenotype of the ES cell-derived *Shox2* cells. We examined expressions of these genes in *Shox2* cells at an early passage (p5), after multiple passages (p48), and in *Shox2* cells cultured as 3D aggregates (p5). The *Shox2* cells p5 expressed several cardiac-specific markers such as α -cardiac actin, myosin light chain MLC-2a, and MLC-2v, confirming their identity as cardiac myocytes (Table 1). The *Shox2* cells showed absent or minimal expression of atrial natriuretic factor (ANF) which is normally expressed at significantly high levels in atrial cardiac myocytes but is absent in pacemaker cells [10, 35]. These cells expressed the pacemaker-specific transcription factors, *Tbx3* at a significantly high level. The expression of *Tbx3* in *Shox2* cells was >400-fold higher than *Nkx2.5*.

Fig. 2 Isolation of the *Shox2* cells and *Cx30.2* cells from EBs. **a** A schematic diagram of the *SHOX2* promoter-*neo* construct used to isolate SA nodal cells. **b** A schematic diagram of the *Cx30.2* enhancer-*neo* construct used to isolate AV nodal cells. **c** A schematic presentation of the method used to isolate pacemaker cells from genetically modified ES cells. **d** A representative phase image of *Shox2* cells proliferating and growing in clusters. **e** A representative *Shox2* cell exhibiting the “spider cell” morphology characteristic of pacemaker cells. **f** A representative phase image of *Cx30.2* cells proliferating in a cluster. **g** A representative *Cx30.2* cell exhibiting the “spider cell” morphology



It is well-known that *Shox2* inhibits *Nkx2.5* expression, and activates a pacemaker genetic pathway that results in the upregulation of *Tbx3* expression [10]. This could explain the marked difference in the expression level of the *Tbx3* and *Nkx2.5* transcripts in the ES cell-derived *Shox2* cells. The transcription factors, *GATA4*, *GATA6*, and myocyte-specific enhancer factor 2C (MEF2C) are expressed early in development [36–38] and were found to be highly expressed in the *Shox2* cells. *Msx2*, a transcription factor that is known for its spatiotemporal and functional correlation with *Tbx2* and *Tbx3* [39], was expressed 30-fold higher than *Nkx2.5*. *Shox2* and its downstream target *BMP4* are abundantly expressed in *Shox2* cells (Table 1). The expression of *BMP4* in *Shox2* cells is 52-fold higher than *BMP2*. Studies have shown that *BMP4* is expressed in the region of the SAN in developing mouse hearts [18], while *BMP2* is essential for the development of the AV canal [40]. The transcription factors, *Tbx3*, *Tbx2*, and *Msx2* maintain the *Shox2* cells in a primitive, undifferentiated state characteristic of pacemaker-nodal cardiac myocytes [41]. We also examined the expression of 15 genes encoding ion channel subunits and

connexins (Cxs). The *Shox2* cells expressed the slow conductance connexins *Cx45* and *Cx30.2* at a high level. These connexins are determinants of the velocity of impulse propagation through the pacemaker tissues, and hence are important contributors to the electrophysiology of the pacemaker cells [42]. The *Shox2* cells also expressed significant levels of genes that are required for generating the rhythmic Ca^{2+} clock and Ca^{2+} dependent depolarizations characteristic of pacemaker-nodal cells. This includes genes encoding the T-type calcium channel subunit gene *Cav3.1*, the L type calcium channel subunits *Cav1.2* and *Cav1.3*, the cardiac ryanodine receptor (*Ryr2*), and the sodium–calcium exchanger (*NCX1*) [25–27, 32, 42–44]. The *Shox2* cells expressed low levels of the cardiac voltage-gated sodium channel (*Nav1.5*) and the inward rectifier potassium channel (*Kir2.1*), which are normally expressed at high levels in working cardiac myocytes but not in pacemaker cells [42, 45, 46]. In addition, we examined the expression of the genes encoding the four hyperpolarization activated cyclic nucleotide gated channel (HCN) isoforms. The HCNs are Na^+/K^+ channels that open at the end of the repolarization phase, when the membrane

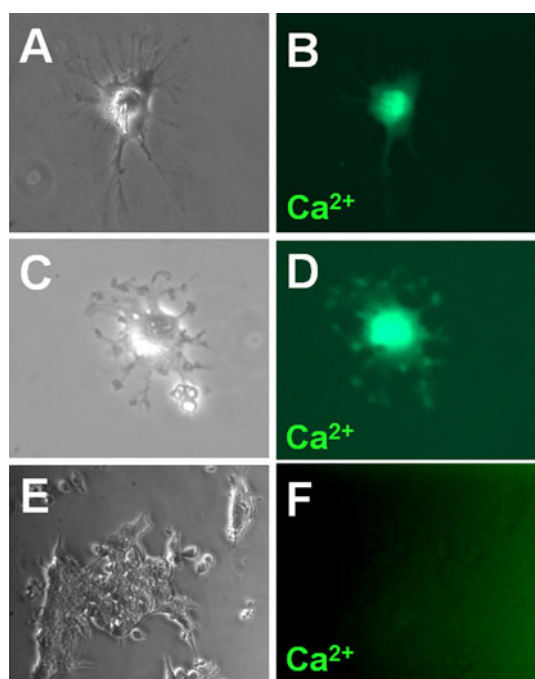


Fig. 3 Calcium imaging of Shox2 cells and Cx30.2 cells. **a** Phase contrast and **b** live fluorescent images of a representative Shox2 cell following fluorescent Ca^{2+} imaging. The Shox2 cell exhibits abundant intracellular Ca^{2+} concentration. **c** Phase contrast and **d** live fluorescent images of a representative Cx30.2 cell following fluorescent Ca^{2+} imaging. The Cx30.2 cell exhibits abundant intracellular Ca^{2+} concentration. **e** Phase contrast and **f** live fluorescent images of a representative cluster of control ES cells following fluorescent Ca^{2+} imaging, showing minimal intracellular Ca^{2+} . Histogram plots of the fluorescence intensity following fluorescent Ca^{2+} imaging in Shox2 cells **g** and Cx30.2 cells **h**, compared to HL-1 cells co-cultured with these cell lines ($n = 4$, $P < 0.01$)

HCN4 (4-fold higher than HCN1), and the HCN3 isoform (3.7-fold higher than HCN1).

In vivo cell therapies are associated with concerns that the cell lines may transdifferentiate giving rise to other cell types, including other cardiac subtypes or even cancerous cells [2, 3] and this can be a serious problem. Accordingly, we have assessed whether the ES cell-derived Shox2 cells and Cx30.2 cells maintained their molecular phenotype after prolonged culture for multiple passages. When we examined the expression of the same 33 genes in Shox2 cells and Cx30.2 cells that have been subjected to multiple passages (p48), we noticed no significant changes in the gene expression compared to early passages (Table 1).

The Shox2 cells were cultured as 3D aggregates in an attempt to generate a critical mass of cells that simulates the in vivo architecture. We compared the gene expression in Shox2 cells p5 cultured as 3D aggregates and Shox2 cells p5 cultured as 2D monolayers. We noticed an increase in the expression levels of the transcription factors, GATA4 (18-fold higher), GATA6 (21.1-fold higher), MEF2C (11-fold higher), Shox2 (3-fold higher), BMP4 (1.5-fold higher), and BMP2 (2-fold higher) in Shox2 cells cultured as 3D aggregates. Moreover, we noticed an increase in the expression levels of several of the important pacemakers channels, including Cav1.3 (2-fold higher), Cav3.1 (37-fold higher), Ryr2 (2-fold higher), NCX1 (64-fold higher), HCN1 (2-fold higher), HCN2 (3-fold higher), HCN3 (2-fold higher), and HCN4 (8-fold higher) in the Shox2 cells cultured as 3D aggregates (Table 1; Supplemental Fig. 1a). These data clearly demonstrate that culturing the ES cell-derived Shox2 cells as 3D aggregates enhanced their pacemaker-nodal phenotype.

Characterization of gene expression profiles in Cx30.2 cells

Using qRT-PCR, we examined the expression of 33 genes in Cx30.2 cells at an early passage (p7), after multiple passages (p48), and in Cx30.2 cells cultured as 3D aggregates (p7). The Cx30.2 cells p7 expressed several cardiac specific markers, such as α -cardiac actin, MLC-2a, and MLC-2v, confirming their identity as cardiac myocytes (Table 1).

potential is very negative (about -60 mV). When these channels open, they allow the slow influx of depolarizing Na^+ ions, resulting in the “funny” current (I_f) which initiates the spontaneous depolarization of the pacemaker cell membrane [47–49]. The Shox2 cells expressed HCN2 at a significant level (16-fold higher than HCN1), followed by

Table 1 Gene expression in ES cell-derived Shox2 cells and Cx30.2 cells

Gene	Shox2p5 (2D)	Shox2 p48 (2D)	Shox2 p5 (3D)	Cx30.2 p7 (2D)	Cx30.2 p48 (2D)	Cx30.2 p7 (3D)
Transcription factors						
1- GATA4	**	**	****	**	**	****
2- GATA6	***	***	****	**	***	***
3- MEF2C	*	*	*	*	*	*
4- Msx2	**	**	***	***	***	***
5- MyoD	*	—	—	*	—	—
6- Nkx2.5	*	*	*	*	*	**
7- Tbx2	***	***	***	***	***	****
8- Tbx3	****	***	****	****	***	****
9- Tbx5	****	*	*	*	*	*
10- Shox2	**	*	***	**	*	**
11- BMP4	****	****	****	****	****	****
12- BMP2	**	*	**	*	**	***
Structural proteins						
13- α -cardiac actin	****	***	****	****	***	****
14- α -skeletal actin	****	****	****	****	****	****
15- Mlc-2a	***	**	****	**	***	**
16- Mlc-2v	***	**	***	*	***	*
17- Desmin	****	****	****	****	***	****
18- ANF	*	*	*	—	—	*
Ion channels and connexins						
19- Cx45	****	****	****	****	****	****
20- Cx30.2	**	*	*	**	**	****
21- Cx43	****	****	****	****	****	****
22- Cx40	—	—	—	—	*	—
23- Cav1.2	*	*	*	—	—	—
24- Cav1.3	*	*	**	*	*	**
25- Cav3.1	*	*	***	*	*	**
26- Ryr2	*	*	**	*	**	*
27- Ncx1	—	*	**	*	*	**
28- Scn5a (Nav1.5)	*	*	*	*	—	*
29- Kir2.1	—	—	*	—	—	*
30- HCN1	*	*	*	*	*	*
31- HCN2	**	**	***	**	*	***
32- HCN3	*	*	*	*	*	*
33- HCN4	*	**	**	*	***	**

Average ($n = 2$). Genes were grouped according to cycle thresholds into the following: ***** <20 ; **** 20–24; *** 24–26; ** 26–28; * > 28 –32; and >32 . See text for definitions of abbreviations

These cells did not express ANF, which is a characteristic of AVN cells [35]. The Cx30.2 cells expressed the pacemaker-specific transcription factors, Tbx3 and Tbx2, at a high level. These transcriptional repressors are known for their major role in suppressing the chamber myocardial phenotype in the region of the AV canal [50, 51]. The expression levels of the transcription factors, GATA4, GATA6, MEF2C, Msx2, BMP4, and BMP2 was high in Cx30.2 cells (Table 1). The transcription factors, Tbx2, Tbx3, and Msx2 help maintain the Cx30.2 cells in a primitive, undifferentiated state

characteristic of pacemaker-nodal cells [41]. In addition, we examined the expression of 15 genes encoding ion channel subunits and connexins. The Cx30.2 cells expressed Cx30.2 at a high level (15-fold higher than Nav1.5). The Cx30.2 cells expressed HCN2 at a significant level (6-fold higher than HCN1), followed by HCN3 (2-fold higher than HCN1). The Cx30.2 cells p5 expressed HCN1 and HCN4 at equal levels (Table 1). The expression of the same 33 genes was assessed in Cx30.2 cells at passage 48 in order to assess whether these cells can maintain their pacemaker-nodal phenotype

following multiple freezing, thawing, and passaging. We noticed no significant change in the gene expression levels with the exception of *BMP2*, *Ryr2*, and *HCN4* which showed a 6-fold, 5-fold, and a 20-fold increase, respectively, when compared to Cx30.2 cells p7 (Table 1).

We cultured Cx30.2 cells as 3D aggregates in an attempt to generate a critical mass of cells that simulates the *in vivo* architecture. We compared the gene expression in Cx30.2 cells p7 cultured as 3D aggregates and Cx30.2 cells p7 cultured as 2D monolayers (Table 1; Supplemental Fig. 1b). We noticed an increase in the expression levels of the transcription factors, GATA4 (14-fold higher), GATA6 (3.5-fold higher), MEF2C (14-fold higher), Msx2 (2-fold higher), Tbx2 (5-fold higher), Tbx3 (2-fold higher), BMP4 (3.5-fold higher), and BMP2 (17-fold higher) in Cx30.2 cells cultured as 3D aggregates. Moreover, we noticed an increase in the expression of several of the important pacemakers connexins and ion channels, including Cx30.2 (12-fold higher), Cav1.3 (5-fold higher), Cav3.1 (12-fold higher), Ryr2 (5-fold higher), NCX1 (5-fold higher), HCN1 (2.5-fold higher), HCN2 (9-fold higher), and HCN4 (4-fold higher) in the Cx30.2 cells cultured as 3D aggregates (Table 1; Supplemental Fig. 1b). These data strongly indicate that culturing the ES cell-derived Cx30.2 cells as 3D aggregates enhanced their pacemaker-nodal phenotype by increasing the expression levels of *Cx30.2* and several ion channels, as well as key cardiovascular regulators of AVN development such as Tbx2, GATA4, and BMP2. The GATA4 transcription factor has been reported to directly activate the expression of the *Cx30.2* gene [14]. This could explain the increase in *Cx30.2* expression level in Cx30.2 cell aggregates. Moreover, GATA transcription factors are also known for activating the expression of several calcium channels [52] including channels that play a role in the intracellular Ca^{2+} release events such as NCX1 and Ryr2 [53]. The increase in GATA4 and GATA6 levels in both the Shox2 and Cx30.2 cell lines could be the cause of the enhanced expression of these calcium channels. The expression of both Tbx2 and BMP2 was upregulated in the Cx30.2 cell 3D aggregates. These two factors have been reported to have interdependent and important roles in the development of the AV canal and the AVN [54]. This upregulation in Tbx2, BMP2, and Cx30.2 expression in Cx30.2 cells confirms their identity as AV nodal cells, since these three factors are major determinants of the development and function of the atrioventricular region in the heart [50, 51, 54–57].

Western analysis of HCN4, connexins, and structural proteins

It is well known that cardiac pacemaker cells rely on the HCNs for the initiation of the spontaneous depolarization wave [48]. HCN4 is the most abundant isoform in cardiac

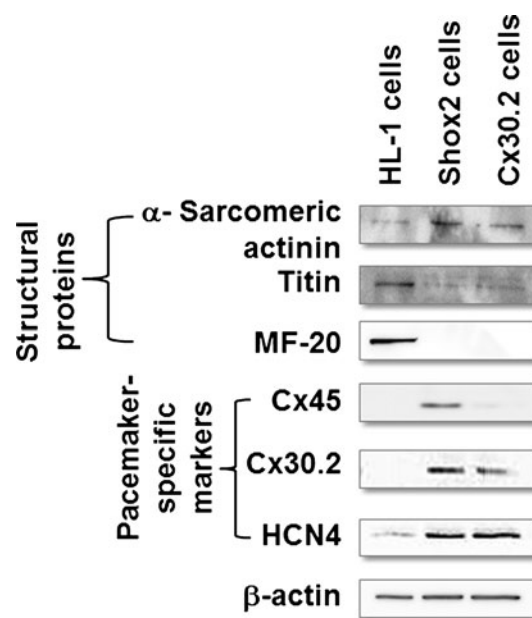


Fig. 4 Characterization of ES cell-derived Shox2 cells and Cx30.2 cells. Western blot analysis of structural and pacemaker-nodal proteins in HL-1 cells, Shox2 cells, and Cx30.2 cells. The structural proteins are α -sarcomeric actinin, titin, and MF20 (Myosin Heavy Chain). The pacemaker-nodal proteins are Cx45, Cx30.2, and HCN4. β -actin was used as loading control

pacemaker cells [58–61]. Using western blot analysis, we demonstrate that Shox2 cells and Cx30.2 cells express abundant levels of HCN4 (Fig. 4). The SA node is characterized by the expression of abundant levels of Cx45 and Cx30.2 proteins [62]. The AV node is characterized by the abundant expression of Cx30.2, which is responsible for the delay that the AV node incorporates between the atrial and ventricular systoles [56, 57]. Our data demonstrate that the Shox2 cells and Cx30.2 cells exhibit a pacemaker-like molecular phenotype and gene expression profile of these connexins (Fig. 4 and Table 1). The Shox2 and Cx30.2 cells exhibited a weak expression of various cardiac structural proteins, which is a molecular phenotype similar to that of primitive cardiac myocytes, and is characteristic of cardiac pacemaker cells [63]. The evaluation of the functionality of these ES cell-derived pacemaker-nodal cell lines in animal models of cardiac pacemaker tissue diseases, such as AV block or sinus node dysfunction, will be required for proof of concept that they would be useful for cell therapy.

Conclusion

Using a genetic selection method, we have identified, isolated, and characterized pure populations of cardiac pacemaker-nodal myocytes that will be useful for the design of biological pacemakers as well as for studying the biology and electrophysiology of these cells.

Acknowledgments We thank Dr. Gudrun Rappold, University of Heidelberg, Germany for the *SHOX2* promoter; Dr. Eric Olson, UT Southwestern for the Cx30.2 enhancer, and Dr. YiPing Chen, Tulane University for CJ-7 (wild type) and *Shox2^{lacZ/+}* ES cells.

References

1. Spooner PM, Albert C, Benjamin EJ, Boineau R, Elston RC, George AL Jr, Jouven X, Kuller LH, MacCluer JW, Marban E, Muller JE, Schwartz PJ, Siscovick DS, Tracy RP, Zareba W, Zipes DP (2001) Sudden cardiac death, genes, and arrhythmogenesis: consideration of new population and mechanistic approaches from a national heart, lung, and blood institute workshop, part I. *Circulation* 103:2361–2364
2. Rosen MR, Brink PR, Cohen IS, Robinson RB (2004) Genes, stem cells and biological pacemakers. *Cardiovasc Res* 64:12–23
3. Rajesh G, Francis J (2006) Biological pacemakers. *Indian Pacing Electrophysiol J* 6:1–5
4. Reinlib L, Field L (2000) Cell transplantation as future therapy for cardiovascular disease?: a workshop of the National Heart, Lung, and Blood Institute. *Circulation* 101:E182–E187
5. Maltsev VA, Rohwedel J, Hescheler J, Wobus AM (1993) Embryonic stem cells differentiate in vitro into cardiomyocytes representing sinusnodal, atrial and ventricular cell types. *Mech Dev* 44:41–50
6. Kehat I, Khimovich L, Caspi O, Gepstein A, Shofti R, Arbel G, Huber I, Satin J, Itskovitz-Eldor J, Gepstein L (2004) Electromechanical integration of cardiomyocytes derived from human embryonic stem cells. *Nat Biotechnol* 22:1282–1289
7. Xue T, Cho HC, Akar FG, Tsang SY, Jones SP, Marban E, Tomaselli GF, Li RA (2005) Functional integration of electrically active cardiac derivatives from genetically engineered human embryonic stem cells with quiescent recipient ventricular cardiomyocytes: insights into the development of cell-based pacemakers. *Circulation* 111:11–20
8. Keith A, Flack M (1907) The form and nature of the muscular connections between the primary divisions of the vertebrate heart. *J Anat Physiol* 41:172–189
9. Ophof T (1988) The mammalian sinoatrial node. *Cardiovasc Drugs Ther* 1:573–597
10. Espinoza-Lewis RA, Yu L, He F, Liu H, Tang R, Shi J, Sun X, Martin JF, Wang D, Yang J, Chen Y (2009) *Shox2* is essential for the differentiation of cardiac pacemaker cells by repressing *Nk2-5*. *Dev Biol* 327:376–385
11. Blaschke RJ, Hahurij ND, Kuijper S, Just S, Wisse LJ, Deissler K, Maxelon T, Anastassiadis K, Spitzer J, Hardt SE, Scholer H, Feitsma H, Rottbauer W, Blum M, Meijlink F, Rappold G, Gittenberger-de Groot AC (2007) Targeted mutation reveals essential functions of the homeodomain transcription factor *Shox2* in sinoatrial and pacemaking development. *Circulation* 115:1830–1838
12. Dobrzynski H, Nikolski VP, Sambelashvili AT, Greener ID, Yamamoto M, Boyett MR, Efimov IR (2003) Site of origin and molecular substrate of atrioventricular junctional rhythm in the rabbit heart. *Circ Res* 93:1102–1110
13. James TN (2003) Structure and function of the sinus node, AV node and his bundle of the human heart: part II-function. *Prog Cardiovasc Dis* 45:327–360
14. Munshi NV, McAnally J, Bezprozvannaya S, Berry JM, Richardson JA, Hill JA, Olson EN (2009) Cx30.2 enhancer analysis identifies *Gata4* as a novel regulator of atrioventricular delay. *Development* 136:2665–2674
15. Klug MG, Soonpaa MH, Koh GY, Field LJ (1996) Genetically selected cardiomyocytes from differentiating embryonic stem cells form stable intracardiac grafts. *J Clin Invest* 98:216–224
16. Jackson M, Taylor AH, Jones EA, Forrester LM (2010) The culture of mouse embryonic stem cells and formation of embryoid bodies. *Methods Mol Biol* 633:1–18
17. White SM, Claycomb WC (2005) Embryonic stem cells form an organized, functional cardiac conduction system in vitro. *Am J Physiol Heart Circ Physiol* 288:H670–H679
18. Puskaric S, Schmitteckert S, Mori AD, Glaser A, Schneider KU, Bruneau BG, Blaschke RJ, Steinbeisser H, Rappold G (2010) *Shox2* mediates *Tbx5* activity by regulating *Bmp4* in the pacemaker region of the developing heart. *Hum Mol Genet* 19:4625–4633
19. White SM, Constantin PE, Claycomb WC (2004) Cardiac physiology at the cellular level: use of cultured HL-1 cardiomyocytes for studies of cardiac muscle cell structure and function. *Am J Physiol Heart Circ Physiol* 286:H823–H829
20. Lam ML, Hashem SI, Claycomb WC (2011) Embryonic stem cell-derived cardiomyocytes harbor a subpopulation of niche-forming Sca-1+ progenitor cells. *Mol Cell Biochem* 349:69–76
21. Livak KJ, Schmittgen TD (2001) Analysis of relative gene expression data using real-time quantitative PCR and the 2(-Delta Delta C(T)) Method. *Methods* 25:402–408
22. DiFrancesco D, Ferroni A, Mazzanti M, Tromba C (1986) Properties of the hyperpolarizing-activated current (if) in cells isolated from the rabbit sino-atrial node. *J Physiol* 377:61–88
23. Verheijck EE, Wessels A, van Ginneken AC, Bourier J, Markman MW, Vermeulen JL, de Bakker JM, Lamers WH, Ophof T, Bouman LN (1998) Distribution of atrial and nodal cells within the rabbit sinoatrial node: models of sinoatrial transition. *Circulation* 97:1623–1631
24. Wu J, Schuessler RB, Rodefeld MD, Saffitz JE, Boineau JP (2001) Morphological and membrane characteristics of spider and spindle cells isolated from rabbit sinus node. *Am J Physiol Heart Circ Physiol* 280:H1232–H1240
25. Mangoni ME, Couette B, Bourinet E, Platzer J, Reimer D, Striessnig J, Nargeot J (2003) Functional role of L-type Cav1.3 Ca²⁺ channels in cardiac pacemaker activity. *Proc Natl Acad Sci USA* 100:5543–5548
26. Mangoni ME, Couette B, Marger L, Bourinet E, Striessnig J, Nargeot J (2006) Voltage-dependent calcium channels and cardiac pacemaker activity: from ionic currents to genes. *Prog Biophys Mol Biol* 90:38–63
27. Marger L, Mesirca P, Alig J, Torrente A, Dubel S, Engeland B, Kanani S, Fontanaud P, Striessnig J, Shin HS, Isbrandt D, Ehmke H, Nargeot J, Mangoni ME (2011) Functional roles of Ca(v)1.3, Ca(v)3.1 and HCN channels in automaticity of mouse atrioventricular cells: insights into the atrioventricular pacemaker mechanism. *Channels (Austin)* 5:251–261
28. Halbach M, Egert U, Hescheler J, Banach K (2003) Estimation of action potential changes from field potential recordings in multicellular mouse cardiac myocyte cultures. *Cell Physiol Biochem* 13:271–284
29. Lakatta EG, Maltsev VA, Bogdanov KY, Stern MD, Vinogradova TM (2003) Cyclic variation of intracellular calcium: a critical factor for cardiac pacemaker cell dominance. *Circ Res* 92:e45–e50
30. Maltsev VA, Vinogradova TM, Lakatta EG (2006) The emergence of a general theory of the initiation and strength of the heartbeat. *J Pharmacol Sci* 100:338–369
31. Bogdanov KY, Maltsev VA, Vinogradova TM, Lyashkov AE, Spurgeon HA, Stern MD, Lakatta EG (2006) Membrane potential fluctuations resulting from submembrane Ca²⁺ releases in rabbit sinoatrial nodal cells impart an exponential phase to the late

- diastolic depolarization that controls their chronotropic state. *Circ Res* 99:979–987
32. Vinogradova TM, Maltsev VA, Bogdanov KY, Lyashkov AE, Lakatta EG (2005) Rhythmic Ca^{2+} oscillations drive sinoatrial nodal cell pacemaker function to make the heart tick. *Ann N Y Acad Sci* 1047:138–156
 33. Vinogradova TM, Lyashkov AE, Zhu W, Ruknudin AM, Sirenko S, Yang D, Deo S, Barlow M, Johnson S, Caffrey JL, Zhou YY, Xiao RP, Cheng H, Stern MD, Maltsev VA, Lakatta EG (2006) High basal protein kinase A-dependent phosphorylation drives rhythmic internal Ca^{2+} store oscillations and spontaneous beating of cardiac pacemaker cells. *Circ Res* 98:505–514
 34. Maltsev VA, Vinogradova TM, Bogdanov KY, Lakatta EG, Stern MD (2004) Diastolic calcium release controls the beating rate of rabbit sinoatrial node cells: numerical modeling of the coupling process. *Biophys J* 86:2596–2605
 35. Habets PE, Moorman AF, Clout DE, van Roon MA, Lingbeek M, van Lohuizen M, Campione M, Christoffels VM (2002) Cooperative action of Tbx2 and Nkx2.5 inhibits ANF expression in the atrioventricular canal: implications for cardiac chamber formation. *Genes Dev* 16:1234–1246
 36. Garg V, Kathiriyai IS, Barnes R, Schluterman MK, King IN, Butler CA, Rothrock CR, Eapen RS, Hirayama-Yamada K, Joo K, Matsuoka R, Cohen JC, Srivastava D (2003) GATA4 mutations cause human congenital heart defects and reveal an interaction with TBX5. *Nature* 424:443–447
 37. Lee Y, Shioi T, Kasahara H, Jobe SM, Wiese RJ, Markham BE, Izumo S (1998) The cardiac tissue-restricted homeobox protein Csx/Nkx2.5 physically associates with the zinc finger protein GATA4 and cooperatively activates atrial natriuretic factor gene expression. *Mol Cell Biol* 18:3120–3129
 38. Adamo RF, Guay CL, Edwards AV, Wessels A, Burch JB (2004) GATA-6 gene enhancer contains nested regulatory modules for primary myocardium and the embedded nascent atrioventricular conduction system. *Anat Rec A Discov Mol Cell Evol Biol* 280:1062–1071
 39. Boogerd KJ, Wong LY, Christoffels VM, Klarenbeek M, Ruijter JM, Moorman AF, Barnett P (2008) Msx1 and Msx2 are functional interacting partners of T-box factors in the regulation of Connexin43. *Cardiovasc Res* 78:485–493
 40. Choi M, Stottmann RW, Yang YP, Meyers EN, Klingensmith J (2007) The bone morphogenetic protein antagonist noggin regulates mammalian cardiac morphogenesis. *Circ Res* 100:220–228
 41. Christoffels VM, Smits GJ, Kispert A, Moorman AF (2010) Development of the pacemaker tissues of the heart. *Circ Res* 106:240–254
 42. Mangoni ME, Nargeot J (2008) Genesis and regulation of the heart automaticity. *Physiol Rev* 88:919–982
 43. Yunker AM, Sharp AH, Sundarraj S, Ranganathan V, Copeland TD, McEnery MW (2003) Immunological characterization of T-type voltage-dependent calcium channel CaV3.1 (alpha 1G) and CaV3.3 (alpha 1I) isoforms reveal differences in their localization, expression, and neural development. *Neuroscience* 117:321–335
 44. Bogdanov KY, Vinogradova TM, Lakatta EG (2001) Sinoatrial nodal cell ryanodine receptor and Na^{+} – Ca^{2+} exchanger: molecular partners in pacemaker regulation. *Circ Res* 88:1254–1258
 45. Miake J, Marban E, Nuss HB (2003) Functional role of inward rectifier current in heart probed by Kir2.1 overexpression and dominant-negative suppression. *J Clin Invest* 111:1529–1536
 46. Wolf CM, Berul CI (2006) Inherited conduction system abnormalities: one group of diseases, many genes. *J Cardiovasc Electrophysiol* 17:446–455
 47. Bucchi A, Barbuti A, DiFrancesco D, Baruscotti M (2012) Funny current and cardiac rhythm: insights from HCN knockout and transgenic mouse models. *Front Physiol* 3:240
 48. Herrmann S, Hofmann F, Stieber J, Ludwig A (2012) HCN channels in the heart: lessons from mouse mutants. *Br J Pharmacol* 166:501–509
 49. Baruscotti M, Bucchi A, Viscomi C, Mandelli G, Consalez G, Gnecci-Rusconi T, Montano N, Casali KR, Micheloni S, Barbuti A, DiFrancesco D (2011) Deep bradycardia and heart block caused by inducible cardiac-specific knockout of the pacemaker channel gene Hcn4. *Proc Natl Acad Sci USA* 108:1705–1710
 50. Singh R, Hoogaars WM, Barnett P, Grieskamp T, Rana MS, Buermans H, Farin HF, Petry M, Heallen T, Martin JF, Moorman AF, 't Hoen PA, Kisper A, Christoffels VM (2012) Tbx2 and Tbx3 induce atrioventricular myocardial development and endocardial cushion formation. *Cell Mol Life Sci* 69:1377–1389
 51. Aanhaanen WT, Brons JF, Dominguez JN, Rana MS, Norden J, Airik R, Wakker V, de Gier-de Vries C, Brown NA, Kispert A, Moorman AF, Christoffels VM (2009) The Tbx2+ primary myocardium of the atrioventricular canal forms the atrioventricular node and the base of the left ventricle. *Circ Res* 104:1267–1274
 52. Wang Y, Morishima M, Zheng M, Uchino T, Mannen K, Takahashi A, Nakaya Y, Komuro I, Ono K (2007) Transcription factors Csx/Nkx2.5 and GATA4 distinctly regulate expression of Ca^{2+} channels in neonatal rat heart. *J Mol Cell Cardiol* 42:1045–1053
 53. Cheng G, Hagen TP, Dawson ML, Barnes KV, Menick DR (1999) The role of GATA, CARG, E-box, and a novel element in the regulation of cardiac expression of the Na^{+} – Ca^{2+} exchanger gene. *J Biol Chem* 274:12819–12826
 54. Yamada M, Revelli JP, Eichele G, Barron M, Schwartz RJ (2000) Expression of chick Tbx-2, Tbx-3, and Tbx-5 genes during early heart development: evidence for BMP2 induction of Tbx2. *Dev Biol* 228:95–105
 55. Harrelson Z, Kelly RG, Goldin SN, Gibson-Brown JJ, Bollag RJ, Silver LM, Papaioannou VE (2004) Tbx2 is essential for patterning the atrioventricular canal and for morphogenesis of the outflow tract during heart development. *Development* 131:5041–5052
 56. Kreuzberg MM, Schrickel JW, Ghanem A, Kim JS, Degen J, Janssen-Bienhold U, Lewalter T, Tiemann K, Willecke K (2006) Connexin30.2 containing gap junction channels decelerate impulse propagation through the atrioventricular node. *Proc Natl Acad Sci USA* 103:5959–5964
 57. Kreuzberg MM, Willecke K, Bukauskas FF (2006) Connexin-mediated cardiac impulse propagation: connexin 30.2 slows atrioventricular conduction in mouse heart. *Trends Cardiovasc Med* 16:266–272
 58. Herrmann S, Layh B, Ludwig A (2011) Novel insights into the distribution of cardiac HCN channels: an expression study in the mouse heart. *J Mol Cell Cardiol* 51:997–1006
 59. Vicente-Stejn R, Passier R, Wisse LJ, Schalij MJ, Poelmann RE, Gittenberger-de Groot AC, Jongbloed MR (2011) Funny current channel HCN4 delineates the developing cardiac conduction system in chicken heart. *Heart Rhythm* 8:1254–1263
 60. Liu J, Dobrzynski H, Gianni J, Boyett MR, Lei M (2007) Organisation of the mouse sinoatrial node: structure and expression of HCN channels. *Cardiovasc Res* 73:729–738

61. Yamamoto M, Dobrzynski H, Tellez J, Niwa R, Billeter R, Honjo H, Kodama I, Boyett MR (2006) Extended atrial conduction system characterised by the expression of the HCN4 channel and connexin45. *Cardiovasc Res* 72:271–281
62. Boyett MR, Inada S, Yoo S, Li J, Liu J, Tellez J, Greener ID, Honjo H, Billeter R, Lei M, Zhang H, Efimov IR, Dobrzynski H (2006) Connexins in the sinoatrial and atrioventricular nodes. *Adv Cardiol* 42:175–197
63. Moorman AF, Christoffels VM (2003) Cardiac chamber formation: development, genes, and evolution. *Physiol Rev* 83:1223–1267